

1 Refining the timing of recombination rate plasticity in
2 response to temperature in *Drosophila*
3 *pseudoobscura*

4 Authors: Ulku H. Altindag¹, Chelsea Shoben², and Laurie S Steverson^{1,*}

5 Affiliations: ¹Department of Biological Sciences, Auburn University, Auburn, AL 36849, USA,

6 ²Biology Department, Duke University, Durham, NC, 27005, *Corresponding Author

7 Email Address: lss0021@auburn.edu

8 Word count: 3936

9 Abstract

10 Meiotic recombination rates vary in response to environmental factors like temperature.
11 Variation in recombination generates an additional source for genetic variation while errors in
12 this pathway can lead to cancer and chromosome number anomalies. Estimating duration and
13 sensitivity of a meiotic response to environmental perturbation requires an understanding of
14 molecular events and well-designed experimental approaches. An earlier study suggested that the
15 peak (most sensitive) timing of plasticity in *Drosophila melanogaster* occurred during the pre-
16 meiotic interphase where DNA replication takes place in S-phase. Recently, heat stress has been
17 shown to lead to plasticity in recombination rates in *D. pseudoobscura*. Here, a combination of
18 molecular genotyping and a series of mutant screens were used to determine peak plasticity
19 timing in this species. Mutant flies were reared in either control or stress temperatures in a
20 traditional cross design. Using mixed model analysis, the odds of crossover formation was 1.53X
21 higher during days 7-9 ($p < 0.0017$) and 1.41X higher on day 9 ($p < 0.022$) in high temperature as
22 compared to control crosses, suggesting the time period as the timing of peak plasticity. Time of
23 peak plasticity at day 9 in *D. pseudoobscura* can be explained by comparison to the model
24 organism *D. melanogaster* due to similar timing of key meiotic events. This comparative
25 approach will enable future mechanistic work on the effects of temperature stress on
26 recombination rate.

27 Introduction

28 Meiosis is fundamental for sexually reproducing organisms to generate haploid gametes. This
29 process helps to maintain the correct number of chromosomes in the next generation, critical for
30 gamete viability. Additionally, crossing over during meiosis creates novel genetic variation by
31 recombining parental haplotypes, which can facilitate adaptation to novel environments. This
32 novel genetic variation due to recombination has important consequences for adaptation of
33 species (Charlesworth & Barton, 1996; Page & Hawley, 2003).

34 Early studies in *Drosophila* have shown that recombination rates vary as a result of exposure to
35 various treatments including maternal age, starvation, humidity, and temperature (Plough, 1917,
36 1921; Bridges, 1927). Over the last century, other model systems have replicated these results
37 (reviewed in (Parsons, 1988; Agrawal *et al.*, 2005; Stevison *et al.*, 2017)). While perturbations
38 have consequences on events throughout meiosis such as in synaptonemal complex and double
39 strand break (DSB) formation, early meiosis appears to be most sensitive to perturbation
40 (Stevison *et al.*, 2017). Experimental evidence points to temperature sensitive pre-meiotic
41 interphase as the stage when recombination rate's plasticity is the highest (Grell, 1973). This
42 coincides with the relationship between meiotic recombination and DNA replication at S-phase
43 (Grell, 1973, 1978b). Grell's studies followed 6 hour transfers to identify the peak timing of
44 recombination due to temperature stress in *D. melanogaster*, to occur at six days following
45 perturbation (Grell, 1973).

46 While there has been a century of work on recombination rate plasticity in *D. melanogaster*,
47 there have been no efforts to document this phenomenon in other *Drosophila* species. *Drosophila*
48 is an extremely diverse genus made up of over 2000 species that diverged over 50 million years
49 ago (Hales *et al.*, 2015). Some have argued that *Drosophila* species can serve as indicators of

50 global climate change (Parsons, 1991). One concern with focusing on *D. melanogaster* in the
51 study of how environmental stress impacts recombination is that it is a cosmopolitan species, and
52 thus may not have the same environmental sensitivity as other species within the *Drosophila*
53 species group. Our team has recently worked to expand research on this ubiquitous phenomenon
54 into *D. pseudoobscura* (Stevison *et al.*, 2017).

55 While traditionally studied for their inversion polymorphisms, *D. pseudoobscura* is native to
56 western North America and a small region in Bogota, Colombia. It is therefore alpine over parts
57 of its range, which means it has the potential to be more sensitive to environmental changes
58 (Kuntz and Eisen, 2014). Additionally, *D. pseudoobscura* females exhibit synchronization of
59 oogenesis across egg chambers (Donald and Lamy, 1938), which is key to studying the timing of
60 events in meiosis because time is an indicator of progression through oocyte development. More
61 recently, there has been a burst of interest in studying recombination rates in this species
62 (Kulathinal *et al.*, 2008, 2009; Stevison and Noor, 2010; McGaugh *et al.*, 2012; Samuk *et al.*,
63 2019).

64 Our lab recently reported a preliminary analysis of recombination rate plasticity due to heat
65 treatment during development in *D. pseudoobscura* (Stevison *et al.*, 2017). In our study, we
66 found significant plasticity in eight regions across the 2nd chromosome, with 5/8 regions
67 showing higher recombination in the high temperature treatment (see Table S1 in Stevison *et al.*
68 2017). These results parallel work done in *D. melanogaster* (Grell, 1966, 1973, 1978a).

69 Here, we continue our work to establish *D. pseudoobscura* as a model for studying
70 recombination rate plasticity. Specifically, we present a series of experiments (summarized in
71 Table 1) aimed at refining the sensitive time period when recombination rate maximally differs
72 in response to temperature. We use a temperature treatment throughout development similar to

73 work of Plough and others (see Figure 2 in (Plough, 1917, 1921; Stevison *et al.*, 2017)). Our
74 previous work used genotyping markers, which showed plasticity along the genome spanning
75 selected mutant markers. The majority of the work described here involves mutant phenotype
76 screens. Combining strategies used in earlier studies, the work we present here will be essential
77 to future mechanistic work to understand the mechanism of recombination rate plasticity and
78 enable it to be studied in more depth in *D. pseudoobscura*.

79 Materials and Methods

80 Stocks

81 Mutant screens were conducted using two X-linked recessive mutant *D. pseudoobscura* stocks.
82 First, a double mutant stock was produced by crossing two lines obtained from the U.C. San
83 Diego stock center (which has relocated to Cornell University): *vermillion* (*v*; 1-88.3) (stock
84 14011-0121.06, Dpse\v[1]) and *yellow* (*y*; 1-74.5) (stock 14044-0121.09, Dpse\y[1]). Our
85 analysis found that the *vermillion* phenotype is most likely *scarlet* (see Results). Mutations of the
86 *vermillion* (and *scarlet*) gene induce a bright red-eye phenotype, and mutations within the *yellow*
87 gene induce a yellow-hued body and wings. Second, a quadruple mutant stock (courtesy of Nitin
88 Phadnis) was used that had four mutations - *yellow* (*y*; 1-74.5), *cut* (*ct*; 1-22.5), *scalloped* (*sd*; 1-
89 43.0), and *sepia* (*se*; 1-156.5) (Phadnis, 2011). Mutations of the *cut* and *scalloped* genes induce
90 changes to the wing phenotype, whereas mutations in the *sepia* gene result in brown eyes.
91 Genetic locations of all mutant markers are shown in Figure 1B. *ct* marker produced inconsistent
92 results due to a variation in penetrance of the *cut* mutation (Dworkin *et al.*, 2009). Therefore, we
93 excluded the *ct-sd* region from the remainder of our analysis.

94 Three wildtype *D. pseudoobscura* stocks were also used for genetic crosses. First, MV2-25 was
95 used with the double mutant stock, which are both in an Arrowhead 3rd chromosome
96 background. Second, AFC-57 (collected in 2015 by K. Ritz from American Fork Canyon, Utah;
97 see (Ritz *et al.*, 2017)) was used for indel genotyping. Finally, to match the 3rd chromosome
98 inversion arrangement of the quadruple mutant stock, a second stock also bearing the
99 arrangement called "Treeline" was obtained from the National Drosophila species Stock Center
100 at Cornell University (stock 14011-0121.265, Dpse\wild-type "TL", SCI_12.2).

101 Husbandry & Cross Design

102 All stocks were maintained at 21°C with a 12 hour light-dark cycle in an incubator. Flies were
103 reared on standard cornmeal–sugar–yeast–agar media in polypropylene enclosures. For indel
104 genotyping, all crosses were performed at 20°C in glass vials containing 6mL of corn syrup food.
105 Virgin female VY flies (5-7 days old) were crossed with male AFC-57. Virgin F₁ females (5-7
106 days old) were collected and crossed with VY male flies. Resulting backcross progeny were
107 phenotyped. Cross design for the SNP genotyping markers was described elsewhere (Stevison *et*
108 *al.*, 2017).

109 Mutant Screens

110 Mutant and wildtype stocks were crossed, and the heterozygous F₁ females were reared in the
111 treatment conditions throughout development (egg-to-adult). F₁ females were backcrossed to
112 wildtype males to ensure no fitness effects associated with recessive mutant alleles. However, for
113 Experiment 3, the backcross was done to the mutant stock. Progeny were screened for
114 recombination frequencies between treatment and control. Crossing schemes for mutant screens
115 are diagrammed in Figure 2 with details on each experimental design outlined in Table 1. Virgin

116 F₁ females were collected within 8 hours after eclosion from the pupal case and held in the
117 control environment for 7 days until reaching full sexual maturity. Males were individually
118 isolated 24 hours prior to crosses to avoid crowding-induced courtship inhibition (Noor, 1997).
119 Backcrosses were conducted as single male and female crosses, with males discarded after 24
120 hours to prevent additional stress from male harassment (Priest, 2007). The vials where virgins
121 were held prior to genetic crosses were kept for 14 days to ensure there were no larvae. If larvae
122 were found, the cross was discarded. To increase sample sizes, multiple backcrosses were
123 conducted from each replicate. Transfer frequency and duration were varied to pinpoint the
124 timing of peak differences in recombination rate due to temperature (see Table 1).
125 Except for Experiment 3, only male progeny were scored and if any female progeny were found
126 to be mutant, the entire vial was discarded and the data removed. Mutant screens recorded each
127 of the mutant traits independently in a single-blind manner. For Experiments 4-5, mutant scoring
128 was delayed at least 5 days for the *sepia* eye color to become more pronounced. Phenotyping
129 ended 2 weeks after eclosion started to prevent the next generation from being included in the
130 data. Every effort was made to score all progeny. However, for Experiments 1-3 this was
131 challenging due to sample sizes that exceeded expectations. For this reason, sample sizes in
132 Table 1 are an underestimate, and fecundity comparisons may be unreliable (see Results). Data
133 were entered in triplicate and compared until 100% concordant.

134 Molecular Genotyping

135 As part of a preliminary characterization of plasticity in *D. pseudoobscura*, Sequenom SNP
136 genotyping markers were designed to genotype crosses between FS14 and FS16 wildtype flies
137 (methods described previously, see Stevison *et al.* 2017). In addition to the chr2 results
138 previously described, seven additional SNP markers were designed on the left arm of the X

139 chromosome (chrXL) to span the region containing the mutant markers *yellow* and *vermillion*
140 (Figure 1A). One marker was excluded based on screens of F₁ progeny, where the marker was
141 completely homozygous, leaving 6 total. Together, the five intervals span 5Mb of the XL and are
142 located on scaffold chrXL_group1e of the *D. pseudoobscura* reference genome.
143 Additionally, two indel markers were designed based on the *D. pseudoobscura* assembly v3.1,
144 each under 25kb from the *vermillion* and *yellow* genes and differing in length between the two
145 stocks (Table S1). DNA was isolated (Gloor and Engels, 1992) from a minimum of 88 flies for
146 each parent stock and backcross progeny for PCR amplification. Length differences for markers
147 were assayed via acrylamide gel. To confirm linkage between the *vermillion* and *yellow* genes
148 and the red eye and yellow body phenotypes, backcross progeny of known phenotype were also
149 genotyped.

150 Statistical Analysis

151 Statistical analysis was performed using R v3.5.2 (R Core Team, 2018). Glm function was
152 used to generate a fitted generalized linear mixed-effects model (GLMM). For each
153 interval within each experiment, a logistic regression analysis with a mixed model was
154 conducted in R. The basic model equation was:

155 *Equation 1:*
$$R = V + D + T + D*T$$

156 R indicates the binary response variable of whether an individual offspring was recombinant or
157 not based on the pair of mutant phenotypes over the screened region. V indicates the replicate
158 vial ID. Individual progeny were summed per replicate vial per day and any vial with fewer than
159 10 progeny were removed to avoid stochasticity in recombination rate estimates. D indicates
160 days post-mating of the F₁ female. Finally, T indicates the temperature in which the F₁ female

161 was reared. For the most part, our interaction terms were not significant, so we extracted
162 individual odds ratios for each time point (Figure 3). For logistic regression, exponentiating
163 the coefficients of GLMM generates the odds of crossover formation between
164 experimental and control conditions.
165 Additionally, to measure the impact of stress due to our treatment, we conducted a linear
166 regression analysis following a similar basic model equation:

167 *Equation 2:*
$$F = V + D + T + D*T$$

168 Here, all variables are the same as Eq. 1, except the response variable, F, in this model is the total
169 number of progeny, fecundity, for each time point. For each replicate vial, fecundity was
170 summed over all crosses and divided by the number of crosses per replicate. The results of both
171 models are summarized in Table 1 and Supplementary Tables 2-3.

172 Results

173 SNP Genotyping markers confirm recombination plasticity of region 174 spanning mutant markers

175 In our earlier molecular analysis, we described results for markers on the 2nd chromosome
176 (Stevison *et al.*, 2017). That analysis also included six X chromosome genetic markers in the
177 region spanning the mutants, *yellow* and *vermillion* (Figure 1A). In analyzing crossover data for
178 intervals 1-3 (shown in black in Figure 3A), we found control crosses had a 12.2%
179 recombination rate, similar to the documented recombination fraction of 14.6 (Anderson 1993).
180 The high temperature crosses had a 16% recombination rate across the same three intervals,
181 which was significantly higher than the control (p=0.019). Across the five intervals, we observed

182 a significant difference in recombination frequency (RF) in intervals 2-4 on days 5-6 and 9-10.
183 There was a peak difference in interval 3 on days 5-6 (Figure 3A). These results confirmed the
184 suitability of this region for use in a mutant screen approach to refine the timing of
185 recombination rate plasticity in response to temperature stress.

186 Initial mutant screens using double mutant stock narrow plasticity to 7-9 187 days

188 We conducted a series of three experiments to pinpoint the timing of differences in
189 recombination rate by crossing a double mutant stock (*yellow* and “*vermillion*”) to the wildtype
190 genome line MV2-25 (Figure 2A). These experiments varied in transfer frequency and duration
191 of progeny collection (Table 1).

192 In Experiment 1, we extended the timeframe of the SNP genotyping experiment from 10 to 20
193 days with 120 hour transfers (Figure 3B). These results did not show any statistically significant
194 differences in RF ($RF_{25}=47.8\%$, $RF_{20}=44.7\%$). Due to our experiment having only a single
195 mating event, the progeny sample sizes for days 16-20 were too small for further consideration.
196 We also shifted the control temperature to the more standard rearing environment of 20°C
197 (Smith, 1958). To maintain a 5°C difference between treatment and control, the temperature
198 treatment was also shifted to 25°C (Table 1).

199 In Experiment 2, we reduced the collections to 15 days and conducted 24 hour transfers. We
200 found several time points had a low sample size with too few replicates and missing data for
201 either treatment or control. Therefore, we aggregated time points for our analysis (Figure 3C).
202 Although we saw minor differences in recombination ($RF_{24.5}=46.7\%$, $RF_{18}=44.3\%$) in days 3-4
203 ($OR=1.48$) and 10-15 ($OR=1.57$), these were not statistically different.

204 Experiment 3 was much larger, with 48-72 hour transfers and backcrosses to the mutant stock
205 rather than wildtype. This resulted in a significant treatment effect in our statistical model
206 ($p=0.02$, Table 1). Additionally, for days 7-9 ($p<0.0017$; $N_{20}=466$; $N_{25}=407$) there was a
207 statistically significant increased odds of observing a crossover at high temperature with
208 $RF_{25}=55.4\%$ and $RF_{20}=45.7\%$ (Fig. 3D). Additionally, days 13-15 were significantly different,
209 but with a large standard error (see Table S3) and small sample size with fewer replicates
210 ($N_{20}=387$; $N_{24}=99$). Thus, we reduced the collection period to 12 days and focused on days 7-9.
211 Rearing temperature did not significantly explain differences in fecundity (Eq. 2) across
212 Experiments 1-3 (Table 1). However, Experiment 1 and 3 showed a decrease in the mean
213 fecundity between temperatures of 17% and 19% respectively (Figure S1).

214 Molecular genotyping reveals *vermillion* mutant is actually *scarlet*

215 In the experiments described above, the recombination fraction calculated between the red eye
216 and yellow body phenotypes were 46%, much higher than the published 14.6%, indicating that
217 one of the mutants was not in the expected gene region. For the indel marker near the *yellow*
218 gene, our results indicated an association between genotype and phenotype (recombination
219 fraction 0/88). However, upon genotyping an indel marker near the *vermillion* gene, we
220 discovered that the bright red eye phenotype did not associate with the indel marker among
221 backcross progeny (recombination fraction 39/85).

222 We then tested whether a mutation in *scarlet* (*st*), another X-linked marker in *D. pseudoobscura*,
223 causes the red-eye phenotype in the progeny. Genotyping confirmed that the bright red eye
224 phenotype was 100% associated with an indel within 21.9kb of the (*st*) gene (recombination
225 fraction 0/471). Sanger sequence analysis revealed a 2bp deletion within the *scarlet* gene of the
226 bright red eyed flies of this strain, suggesting a frame-shift mutation within the *scarlet* gene is a

227 likely cause for this phenotype. Although there is not a consistent map location for *scarlet* in the
228 literature in *D. pseudoobscura* (Beers, 1937; Mampell, 1943), it is consistently 30cM away from
229 *sepia* (Figure 1B). This places it roughly 52cM away from *yellow*, consistent with our observed
230 recombination rates.

231 Mutant screens using quadruple mutant stock pinpoint 9 day peak in 232 plasticity

233 Once we confirmed the double mutant stock contained markers that were >50cM apart, we
234 obtained a quadruple mutant stock to continue mutant screens (Figure 2B). We conducted two
235 additional experiments to refine the timing of recombination rate plasticity.
236 Our results in Experiments 4-5 for the *sd-y* region (38.5%) closely matched the expected rate
237 (32.5%). Similar to *y-st*, the *y-se* region had a large recombination rate (46.4%) consistent with
238 the genetic map distance (82cM). However, the results for the *ct-sd* region (6%) were
239 substantially lower than expected (20.5%), thus we excluded the *ct-sd* region from our analysis
240 (see Methods). In Experiment 4, the highest odds ratios were observed on days 4-6 for the *sd-y*
241 region (1.24) and on days 10-12 for the *y-se* region (1.107, Figure 3E), though none of these
242 results were significant. Still, based on the results from Experiment 3 in days 7-9, we focused on
243 this time period with 24 hour transfers. In Experiment 5, the highest odds ratio was observed on
244 day 9 (1.41) in the *y-sd* region (Fig. 3F, $p=0.035$, $N_{21}=630$ and $N_{26}=296$). The total
245 recombination across the *sc-se* region was also significant on day 9 (Table S3, $p=0.022$).
246 Similarly, the median RF across replicates for this time point was 26% at 21°C and 29% at 26°C
247 (Figure 4).

248 In Experiments 4-5, temperature had a significant effect on fecundity (Table 1, Supplementary
249 Figure 1), with a decrease in the treatment group. For Experiment 4, there was a 51% decrease in
250 mean fecundity due to temperature ($p < 0.0001$, see Table 1). In Experiment 5 average fecundity
251 from days 6-10 in the control and experimental conditions were 20.9 and 15.0, respectively
252 ($p < 0.019$).

253 Discussion

254 Our results in Experiment 3 narrowed the timing of recombination rate plasticity in response to
255 heat stress to 7-9 day post-mating. The double mutant stock was then found to have markers that
256 were 52cM apart rather than our expected 14.6cM distance. Therefore, we used a quadruple
257 mutant stock to further narrow the timing of the peak difference in recombination rate due to
258 temperature as day 9 post mating in Experiment 5. Interestingly, declined fecundity due to heat
259 stress was only significantly different in Experiments 4-5 (Figure S1) where the temperature
260 stress was at 26°C (maximum of the species range, (Kuntz and Eisen, 2014). We also found a
261 significant correlation between fecundity and recombination rate among the replicates for day 9
262 in Experiment 5 (Figure S2B) in both the control ($p_{Exp5} = 0.04$) and treatment ($p_{Exp5} = 0.02$). This
263 was not the case for days 7-9 in Experiment 3 (Figure S2A).

264 Another interesting finding was that the region spanning the centromere and out into XR (*y-v*; *y-*
265 *se*) appears to have a peak recombination difference due to temperature slightly earlier. This
266 finding matches previous experiments in *D. melanogaster*, which showed that regions near the
267 centromere were affected by varying environmental conditions (Grell, 1973). For example, the
268 SNP genotyping had a peak odds ratio of 6.97 on days 5-6 for the region between m_3 and m_4 (Fig
269 3A). Similarly, in Experiment 5, the interval *y-se* had a peak odds ratio of 1.29 on day 6 (Figure

270 3F, NS), as compared to the *sd-y* which peaked on day 9 (Figure 4). This finding suggests the
271 timing of plasticity varies spatially along the genome as well as over time, not unlike the findings
272 of Grell (Grell, 1973). A more comprehensive genome-wide study would be useful to understand
273 the genomic properties that contribute to this spatial variation.
274 Finally, we show that our results are reproducible by summing data over multiple days from the
275 24 hour experiments, we compared them to the multi-day transfers. Results between Experiments
276 4 and 5 were highly concordant and within the 95% CI for intervals *y-sd* and *y-se* (Figure S3).
277 However, for the interval *y-st* between Experiments 2 and 3, they were not overlapping. This is
278 likely due to issues with Experiment 2 given the lack of progeny in several time points (see
279 Results).

280 Peak plasticity at day nine points to events in early meiosis

281 The physiological processes influencing recombination rate need to be further explored.
282 Although there has been a lot of work done in *D. melanogaster*, there are other *Drosophila*
283 species that may be more sensitive to environmental perturbations for studying this important
284 phenomenon. For example, cactophilic (Markow, 2019) and mushroom feeding (Scott Chialvo *et*
285 *al.*, 2019) *Drosophila* represent recent adaptive radiations with growing potential for ecological
286 genomics. Additionally, the *montium* species group has recently become genome-enabled and is
287 well suited for testing various evolutionary hypotheses (Bronski *et al.*, 2020).
288 Here, we have examined plasticity in the alpine species, *D. pseudoobscura*. Exchange between
289 homologous chromosomes starts in the early pre-meiotic stages and are not yielded as crossing
290 over until metaphase I in all eukaryotes (Page and Hawley, 2003). In *D. melanogaster*,
291 development from oogenesis to egg maturation takes 10 days and a fully matured oocyte is

292 selected in stages 1-14 in the last 79 hours (Koch and King, 1966). Although, *D. pseudoobscura*
293 oogenesis remains understudied, *Drosophila* species respond to temperature in a distinct manner.
294 Moreover, the decrease in developmental time due to increased temperature is muted in alpine
295 species such as *D. pseudoobscura* (Kuntz and Eisen, 2014). For example, in Experiment 4, we
296 saw a 3-4 day shorter development time in the high temperature treatment as compared to the
297 control.

298 Moreover, crossover formation varies in the same way as different phenotypes are influenced by
299 physiological factors. Developmental events such as invagination of the cephalic fold in stage 8
300 and retracting of the germband in stage 13 of oogenesis happen faster in high temperature in *D.*
301 *pseudoobscura*. The gene *recombination defect (rec)* was identified by Grell in temperature
302 sensitive mutants of *D. melanogaster*, is involved in generating meiotic crossovers, and DNA
303 double strand break (DSB) formation (Grell, 1984). Later studies in *D. pseudoobscura* examined
304 the protein encoded by the *rec* gene, MCM8 showed it was evolutionarily conserved. This
305 protein complex contributes to the stability of DNA strands during DSB and synaptonemal
306 complex formation, and is transcribed early in developmental stages (Hunter, 2015). In
307 *Drosophila* these events take place concurrently and affect regulation of crossovers (Carpenter,
308 1975). The protein complexes common in these processes show a temporal pattern that can be
309 tracked by developmental stages. Grell's work in *D. melanogaster* showed that all three
310 processes were present in 16 cell cyst in the adult flies by 6 days pinpointing the peak plasticity
311 at the same time. While our experimental design is quite different from Grell's work, it is worth
312 noting that in *D. pseudoobscura*, late replication domains are present in the early stages of
313 oogenesis, indicating the S-phase occurs after day 8 post mating coinciding with the observed

314 peak in recombination rate plasticity in this study (Higgins *et al.*, 2012; Andreyenkova *et al.*,
315 2013).

316 Acknowledgements

317 This work was supported by research start-up funds to LSS from the Department of Biological
318 Sciences at Auburn University. UHA was supported by NSF-DEB EAGER No. 1939090 to LSS.
319 We thank members of the Noor Lab for generating the double mutant VY stock used for
320 Experiments 1-3. We thank Mohamed Noor for guidance and feedback on this work. We thank
321 the Graze lab for help with fly husbandry for experiments 1-3, which were conducted in the fly
322 lab of Rita Graze of Auburn University. We thank the Phadnis Lab for sharing the quadruple
323 mutant stock used for Experiments 4-5. We thank Todd Steury for consultation on our statistical
324 analysis. We thank members of the Stevison Lab for extensive help with mutant phenotype
325 screens, with particular thanks to Natalia Rivera-Rincon, Keeley Pownall, Neeve Curley, Kyle
326 Meding, Hannah Taylor, Anna Tourne, Adam King, Kaitlyn Walter, and several other
327 undergraduate researchers over a three year period.

328 Conflict of Interest

329 Authors state that there is no conflict of interest.

330 Data Availability

331 Data files and scripts to complete the analysis are available on github
332 (<https://github.com/StevisonLab/Peak-Plasticity-Project>). Also, we have included a walk through
333 tutorial for the analysis of data in Experiment 3 in R markdown.

334 References

- 335 Agrawal AF, Hadany L, Otto SP (2005). The Evolution of Plastic Recombination. *Genetics* **171**:
336 803–812.
- 337 Andreyenkova NG, Kolesnikova TD, Makunin IV, Pokholkova GV, Boldyreva LV, Zykova TY,
338 *et al.* (2013). Late Replication Domains Are Evolutionary Conserved in the *Drosophila*
339 Genome. *PLOS ONE* **8**: e83319.
- 340 Beers CV (1937). Linkage Groups in *Drosophila Pseudoobscura*, Race B. *Genetics* **22**: 577–586.
- 341 Bridges CB (1927). THE RELATION OF THE AGE OF THE FEMALE TO CROSSING
342 OVER IN THE THIRD CHROMOSOME OF *DROSOPHILA MELANOGASTER*. *J*
343 *Gen Physiol* **8**: 689–700.
- 344 Bronski MJ, Martinez CC, Weld HA, Eisen MB (2020). Whole Genome Sequences of 23
345 Species from the *Drosophila montium* Species Group (Diptera: Drosophilidae): A
346 Resource for Testing Evolutionary Hypotheses. *G3 Genes Genomes Genet.*
- 347 Carpenter ATC (1975). Electron microscopy of meiosis in *Drosophila melanogaster* females: I.
348 Structure, arrangement, and temporal change of the synaptonemal complex in wild-type.
349 *Chromosoma* **51**: 157–182.
- 350 Charlesworth B, Barton NH (1996). Recombination load associated with selection for increased
351 recombination. *Genet Res* **67**: 27–41.
- 352 Donald HP, Lamy R (1938). VI.—Ovarian Rhythm in *Drosophila*. *Proc R Soc Edinb* **57**: 78–96.
- 353 Gloor GB, Engels WR (1992). From: Single–Fly DNA Preps for PCR. *Drosoph Inf Serv* **71**:
354 148–149.
- 355 Grell RF (1966). The Meiotic Origin of Temperature-Induced Crossovers in *DROSOPHILA*
356 *MELANOGASTER* Females. *Genetics* **54**: 411–421.

- 357 Grell RF (1973). RECOMBINATION AND DNA REPLICATION I N THE DROSOPHILA
358 MELANOGASTER OOCYTE. : 22.
- 359 Grell RF (1978a). High frequency recombination in centromeric and histone regions of
360 Drosophila genomes. *Nature* **272**: 78–80.
- 361 Grell RF (1978b). Time of recombination in the Drosophila melanogaster oocyte: evidence from
362 a temperature-sensitive recombination-deficient mutant. *Proc Natl Acad Sci* **75**: 3351–
363 3354.
- 364 Grell RF (1984). Time of recombination in the Drosophila melanogaster oocyte. III. Selection
365 and characterization of temperature-sensitive and-insensitive, recombination-deficient
366 alleles in Drosophila. *Genetics* **108**: 425–443.
- 367 Hales KG, Korey CA, Larracuente AM, Roberts DM (2015). Genetics on the Fly: A Primer on
368 the Drosophila Model System. *Genetics* **201**: 815–842.
- 369 Higgins JD, Perry RM, Barakate A, Ramsay L, Waugh R, Halpin C, *et al.* (2012).
370 Spatiotemporal Asymmetry of the Meiotic Program Underlies the Predominantly Distal
371 Distribution of Meiotic Crossovers in Barley. *Plant Cell* **24**: 4096–4109.
- 372 Hunter CM (2015). Environmental and Genetic Determinants of Recombination Rate in
373 Drosophila melanogaster. Ph.D. Thesis, North Carolina State University.
- 374 Kulathinal RJ, Bennett SM, Fitzpatrick CL, Noor MAF (2008). Fine-scale mapping of
375 recombination rate in Drosophila refines its correlation to diversity and divergence. *Proc*
376 *Natl Acad Sci* **105**: 10051–10056.
- 377 Kulathinal RJ, Stevison LS, Noor MAF (2009). The Genomics of Speciation in Drosophila:
378 Diversity, Divergence, and Introgression Estimated Using Low-Coverage Genome
379 Sequencing. *PLoS Genet* **5**.

- 380 Kuntz SG, Eisen MB (2014). *Drosophila* Embryogenesis Scales Uniformly across Temperature
381 in Developmentally Diverse Species. *PLoS Genet* **10**.
- 382 Mampell K (1943). Genetic Studies in *Drosophila Pseudoobscura*. PhD Thesis, California
383 Institute of Technology.
- 384 Markow TA (2019). Ecological and Evolutionary Genomics: The Cactophilic *Drosophila* Model
385 System. *J Hered* **110**: 1–3.
- 386 McGaugh SE, Heil CSS, Manzano-Winkler B, Loewe L, Goldstein S, Himmel TL, *et al.* (2012).
387 Recombination Modulates How Selection Affects Linked Sites in *Drosophila*. *PLOS Biol*
388 **10**: e1001422.
- 389 Noor MAF (1997). Environmental effects on male courtship intensity in *Drosophila*
390 *pseudoobscura* (Diptera: Drosophilidae). *J Insect Behav* **10**: 305–312.
- 391 Page SL, Hawley RS (2003). Chromosome Choreography: The Meiotic Ballet. *Science* **301**:
392 785–789.
- 393 Parsons PA (1988). Evolutionary rates: effects of stress upon recombination. *Biol J Linn Soc* **35**:
394 49–68.
- 395 Parsons PA (1991). Biodiversity Conservation Under Global Climatic Change: The Insect
396 *Drosophila* as a Biological Indicator? *Glob Ecol Biogeogr Lett* **1**: 77–83.
- 397 Phadnis N (2011). Genetic Architecture of Male Sterility and Segregation Distortion in
398 *Drosophila pseudoobscura* Bogota–USA Hybrids. *Genetics* **189**: 1001–1009.
- 399 Plough HH (1917). The effect of temperature on crossingover in *Drosophila*. *J Exp Zool* **24**:
400 147–209.
- 401 Plough HH (1921). Further studies on the effect of temperature on crossing over. *J Exp Zool* **32**:
402 187–202.

- 403 Priest (2007). MATING-INDUCED RECOMBINATION IN FRUIT FLIES - Priest - 2007 -
404 Evolution - Wiley Online Library.
- 405 R Core Team (2018). *R: A language and environment for statistical computing*. R Foundation for
406 Statistical Computing, Vienna, Austria.
- 407 Ritz KR, Noor MAF, Singh ND (2017). Variation in Recombination Rate: Adaptive or Not?
408 *Trends Genet* **33**: 364–374.
- 409 Samuk K, Manzano-Winkler B, Ritz KR, Noor MAF (2019). Natural selection shapes variation
410 in genome-wide recombination rate in *Drosophila pseudoobscura*. *bioRxiv*: 787382.
- 411 Scott Chialvo CH, White BE, Reed LK, Dyer KA (2019). A phylogenetic examination of host
412 use evolution in the quinaria and testacea groups of *Drosophila*. *Mol Phylogenet Evol*
413 **130**: 233–243.
- 414 Smith JM (1958). The Effects of Temperature and of Egg-Laying on the Longevity of
415 *Drosophila Subobscura*. *J Exp Biol* **35**: 832–842.
- 416 Stevison LS, Noor MAF (2010). Genetic and Evolutionary Correlates of Fine-Scale
417 Recombination Rate Variation in *Drosophila persimilis*. *J Mol Evol* **71**: 332–345.
- 418 Stevison LS, Sefick S, Rushton C, Graze RM (2017). Recombination rate plasticity: revealing
419 mechanisms by design. *Philos Trans R Soc B Biol Sci* **372**: 20160459.
- 420 Sturtevant AH, Tan CC (1937). The comparative genetics of *Drosophila pseudoobscura* and
421 *melanogaster*. *J Genet* **34**: 415–432.

422 Figure Legends

423 **Figure 1. Physical and genetic location of markers used to measure recombination**

424 **frequency in *D. pseudoobscura*.** (A) Physical locations of SNP genotyping markers along 12.5

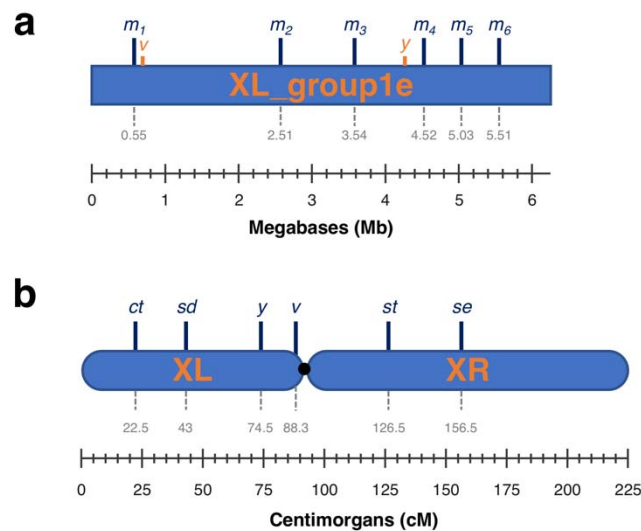
425 Mb scaffold “XL_group1e” located on the left arm of the X chromosome (XL). This scaffold

426 covers 62% of XL, including the mutant markers *yellow* and *vermillion*. (B) Genetic map of X

427 chromosome with location of mutant X-linked markers for recombinant screens. The majority of

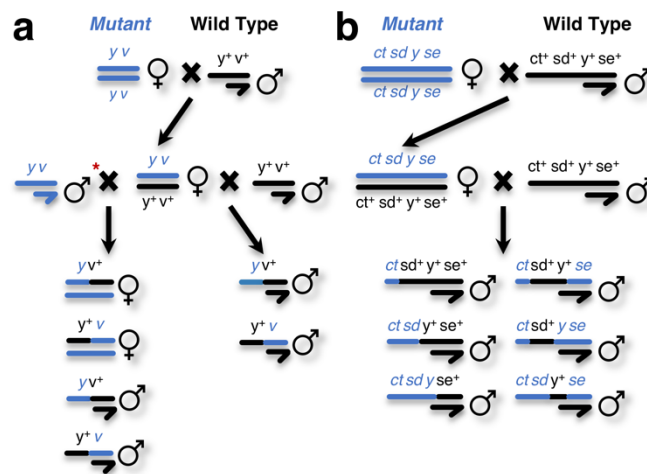
428 markers were located on the XL. It was later discovered that our presumed *vermillion* marker in

429 experiments 1-3 was actually *scarlet* (also shown).



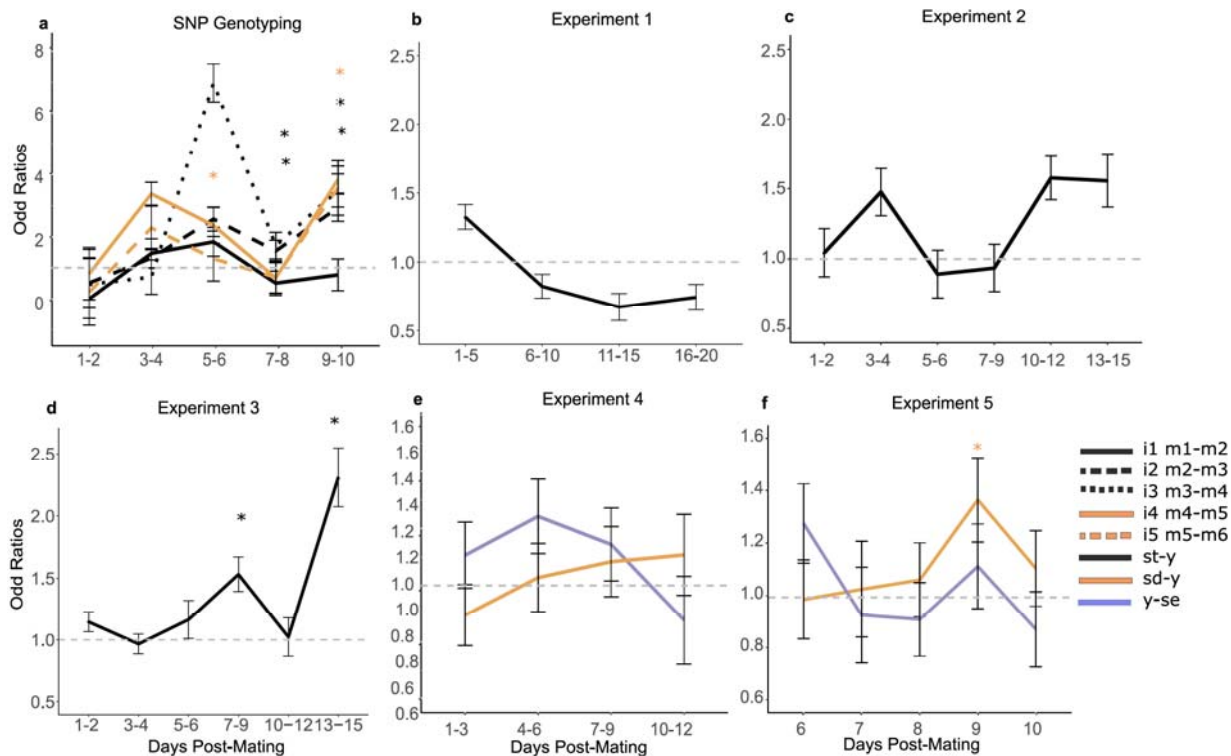
430

431 **Figure 2. Crossing scheme for mutant phenotype screens.** Females homozygous for mutant
 432 markers of two stocks were used to cross to wildtype flies. In Experiments 1-3, the *y-v* mutant
 433 stock and the MV2-25 wildtype stock were used (A). In Experiments 1 and 2, F₁ females were
 434 backcrossed to the wildtype stock, whereas in Experiment 3, F₁ females were backcrossed to the
 435 mutant stock (indicated by red asterisk). For Experiments 4-5, the quadruple mutant stock *ct-sd-*
 436 *y-se* and the SCI_12.2 wildtype stock were used (B). Based on initial screening of male progeny,
 437 the marker *ct* was removed from consideration as it gave unreliable results due to incomplete
 438 penetrance. Male progeny were screened for recombination analysis (Eq. 1) and female progeny
 439 were counted for fecundity analysis (Eq. 2).



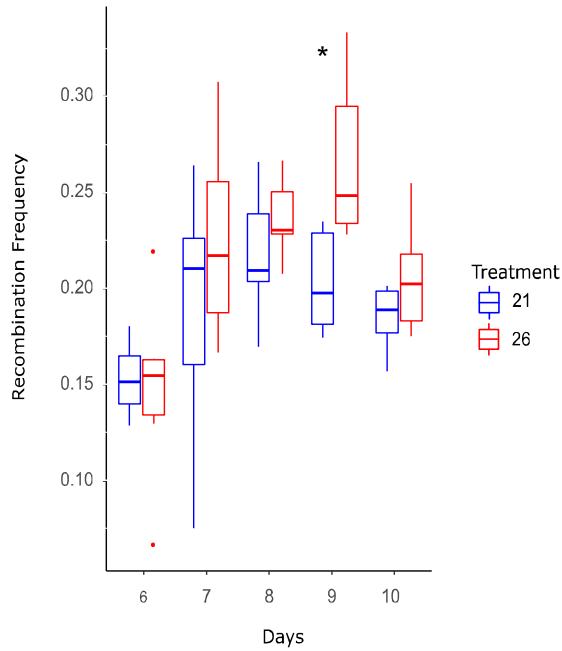
440

441 **Figure 3. Recombination results for SNP genotyping and mutant screening Experiments 1-**
 442 **5.** Recombination frequencies between control and treatment were compared using a fitted
 443 generalized linear mixed-effects model (GLMM). Exponentiating the coefficients generated the
 444 odds ratio. Odds ratios across experiments were plotted against days post-mating and indicate the
 445 odds of having a crossover in high temperature compared to control. (A) Odds ratios for the SNP
 446 genotyping markers. (B-D) Odds ratios for the double mutant screens in the *y-v* region, and (E-F)
 447 odds ratios for the quadruple mutant screens in the intervals *sd-y* (red) and *y-se* (blue). A post
 448 hoc test was done to calculate significance for each timepoint between treatment and control with
 449 significance indicated via asterisks (see Table S3). See Table 1 for additional details regarding
 450 differences in experimental design across panels.



451

452 **Figure 4. Recombination rates across interval *sd-y* over 24h periods from Experiment 5.** As
453 in Figure 3F, day 9 shows a significant difference in recombination rate (*p=0.035) between the
454 control (green) and high temperature (purple) for the interval between *scalloped* and *yellow*. The
455 boxplots show variation in recombination rate among the six replicates per treatment.



456

457 Table Legends

458 **Table 1. Summary of experimental design for series of genotyping experiments to measure**
 459 **the impact of temperature on recombination frequency.** For each experiment, a different set
 460 of temperatures, transfer frequencies and duration as well as sample sizes were used. *Note:
 461 Sample size is based only on the number of individuals targeted for recombination frequency.
 462 (e.g. only males were phenotyped for Exp 1, 2, 4, and 5). For fecundity, values are based on all
 463 progeny of both sexes for the duration of the experiment but not over the lifetime of each
 464 replicate female. For transfer frequency and duration, H denotes hours and D denotes days. □P-
 465 value from Eq. 2 for Treatment on Fecundity. □P-value from Eq. 1 for Treatment on
 466 Recombination Rate. Full anova tables for both analyses are in Table S2. ^aCrossing scheme
 467 matches Figure 2A. ^bCrossing scheme matches Figure 2B.

	Transfer frequency/duration	# rep vials/treatment	Median # crosses/rep	Temperatures	Sample Size*	Fecundity[□]	Recombination[□]
SNP Genotyping	48H/10D	4/4	4/4	18°C/23°C	677/611	n/a	0.29
Experiment 1^a	120H/20D	4/5	8/6	20°C/25°C	678/529	0.36	0.71
Experiment 2^a	24H/15D	4/4	9/8	18°C/24.5°C	1080/887	0.43	0.23
Experiment 3^a	48H/6D; 72H/6-15D	8/9	10/10	20°C/25°C	5205/4488	0.24	0.02
Experiment 4^b	72H/12D	5/5	5/5	21°C/26°C	4140/2071	5.54E-08	0.67
Experiment 5^b	24H/6-10D	6/6	12/12	21°C/26°C	3425/2084	4.49E-04	0.88

468